

## Proton hole states of $^{95,97,99}\text{Nb}^\dagger$

P. K. Bindal, D. H. Youngblood, and R. L. Kozub\*

Cyclotron Institute and Physics Department, Texas A & M University, College Station, Texas 77843

(Received 15 April 1974)

The  $(d, {}^3\text{He})$  reactions on  $^{96,98,100}\text{Mo}$  have been used at 40.7 MeV bombarding energy to populate proton hole states in the Nb isotopes. Ten groups of levels were observed in each nucleus and most of the expected strength in the  $1g_{9/2}$ ,  $2p_{1/2}$ ,  $2p_{3/2}$ , and  $1f_{5/2}$  orbits was observed. Excitation energies and  $l$  values were obtained for nine new excited levels in  $^{99}\text{Nb}$ . The  $Q$  value for the  $^{100}\text{Mo}(d, {}^3\text{He})^{99}\text{Nb}$  reaction was measured to be  $-5.639 \pm 0.015$  MeV, giving a  $^{99}\text{Nb}$  mass excess of  $-82\,342 \pm 15$  keV. A hole-core coupling model is used to predict the levels of the Nb isotopes, and fair agreement with experiment is obtained.

NUCLEAR REACTIONS, NUCLEAR STRUCTURE  $^{96,98,100}\text{Mo}(d, {}^3\text{He})$ ,  $E = 40.7$  MeV; measured  $\sigma(\theta)$ ,  $^{100}\text{Mo}(d, {}^3\text{He})$   $Q$  value;  $^{95,97,99}\text{Nb}$  levels deduced  $l$ ,  $S$ ,  $\pi$ ,  $^{99}\text{Nb}$  mass excess; calculated  $J$ ,  $\pi$ ,  $S$ , particle-core-coupling model, predicted  $Q_{2+}$  for  $^{96,98,100}\text{Mo}$ .

### I. INTRODUCTION

In recent years, although there have been several experimental studies<sup>1-5</sup> of the proton configurations of nuclei in the  $A = 90-100$  region, theoretical interest has been limited. Proton pickup reactions on Mo isotopes<sup>1</sup> and Zr isotopes<sup>3</sup> revealed little change in proton configuration as neutrons were added to the  $2d_{5/2}$  shell. Little information existed on the ground state wave function of  $^{100}\text{Mo}$  where neutrons are naively in the  $3s_{1/2}$  shell. In addition, it has been recently suggested<sup>6</sup> that  $^{100}\text{Mo}$  is a transitional nucleus, with a new deformed region around  $A \approx 104-106$ . Although considerable information exists on the level structure of the lighter Nb isotopes, only scant information was available for  $^{99}\text{Nb}$ , obtained by measurement of  $\gamma$ -decay schemes following  $^{99}\text{Zr}$   $\beta$  decay.<sup>7</sup>

The only information available for the low-lying proton hole states in the Nb isotopes is from the study of Ohnuma and Yntema.<sup>1</sup> Our recent study of hole state analogs of Nb levels in the Mo isotopes<sup>8</sup> revealed a dramatic drop in analog state strength, particularly for  $l = 1$  states as one progresses to higher Mo isotopes, even though the results of Ref. 1 indicate that the parent state strength is essentially constant up through  $^{95}\text{Nb}$  and drops only slightly in  $^{97}\text{Nb}$ . The  $(d, {}^3\text{He})$  reactions on  $^{96,98}\text{Mo}$  were studied to supplement the data of Ohnuma and Yntema, who studied the  $^{91,93,95,97}\text{Nb}$  nuclei with the same reaction at much lower bombarding energy (23 MeV). The  $^{100}\text{Mo}(d, {}^3\text{He})^{99}\text{Nb}$  reaction was also studied to provide additional structure information about the  $^{100}\text{Mo}$  and  $^{99}\text{Nb}$  nuclei and to obtain parent state spectroscopic factors for a continuation of the work described in Ref. 8.

Calculations by Bhatt and Ball<sup>9</sup> and Vervier<sup>10</sup>

predict energy levels for the Nb isotopes assuming proton occupation of the  $p_{1/2}$  and  $g_{9/2}$  orbitals with a  $^{88}\text{Sr}$  closed core. Some success has been attained in predicting<sup>11</sup> the negative parity hole states of  $^{99}\text{Nb}$  with a core-coupling model. The low-lying proton hole states of the odd- $A$  Nb nuclei can be described by two types of models in which the even-even Mo nuclei are coupled to proton holes which may occupy the  $2p_{1/2}$ ,  $2p_{3/2}$ , and  $1f_{5/2}$  shell model orbits. In the first model, the hole-phonon model, the basic states of the core are assumed to be the quadrupole oscillations of a quantized liquid drop, while in the second model, the hole-core model, only a few basic states of the core are considered, which are eigenfunctions of a core Hamiltonian for which no explicit form is assumed. We take the second model for the calculations in this paper since it is both conceptually simple and yet capable of considerable generality. In a later communication<sup>12</sup> we shall present results of the hole-phonon model where effects of dissociation of phonons into particle-hole pairs will be included.

The experimental procedure is briefly discussed in Sec. II, while the distorted-wave Born-approximation (DWBA) analysis is discussed in Secs. III and IV. Section V is a brief discussion of the hole-core-coupling model used to predict the energy levels,  $J^\pi$  values, and the spectroscopic factors. The results are summarized and compared with the experimental data in Sec. VI.

### II. EXPERIMENTAL PROCEDURE

The experimental details are similar to those described previously.<sup>2</sup> A 40.7 MeV deuteron beam from the Texas A & M cyclotron was used to bombard self-supporting  $^{96,98,100}\text{Mo}$  foils en-

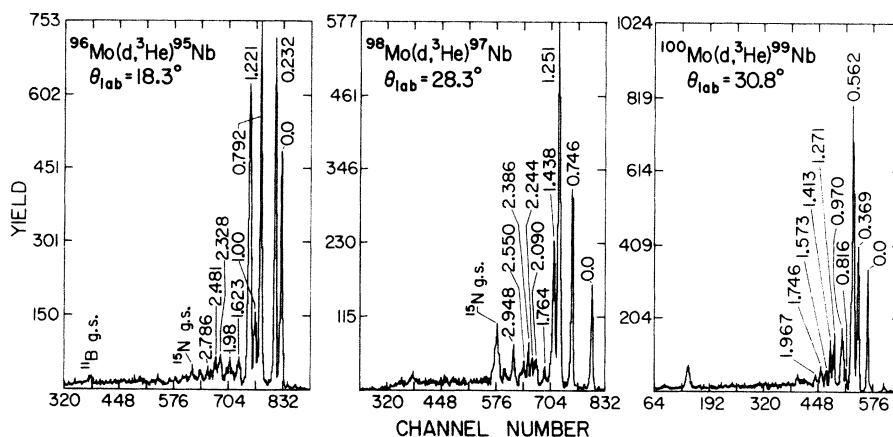


FIG. 1. The spectra of the  $^{96,98,100}\text{Mo}(d,^3\text{He})^{95,97,99}\text{Nb}$  reactions. The excitation energies of observed states are indicated in MeV.

riched to greater than 95% in the desired isotope. The targets were approximately  $600 \mu\text{g}/\text{cm}^2$  thick, with thicknesses determined by weighing. Two silicon detector telescopes spaced  $5^\circ$  apart were used simultaneously, and selected data points were checked by measurements with both systems. The telescopes consisted of  $500 \mu\text{m} \Delta E$ ,  $3\text{mm} E$ , and  $1.5 \text{mm}$  veto detectors for the forward stack with  $200 \mu\text{m} \Delta E$ ,  $1 \text{mm} E$ , and  $700 \mu\text{m}$  veto detec-

tors for the other stack. The veto detector served to eliminate pulses due to the elastically scattered deuterons. Helion ( $^3\text{He}$ ) and triton ( $^3\text{H}$ ) pulses were selected using power law identifier circuits for each telescope and the total energy pulses were routed into analog to digital converters interfaced to the IBM 7094 computer. Helion spectra from each of the targets are shown in Fig. 1 and extend to an excitation energy of 8 MeV. The overall resolution obtained was about 50 keV full width at half maximum. The triton data will be included

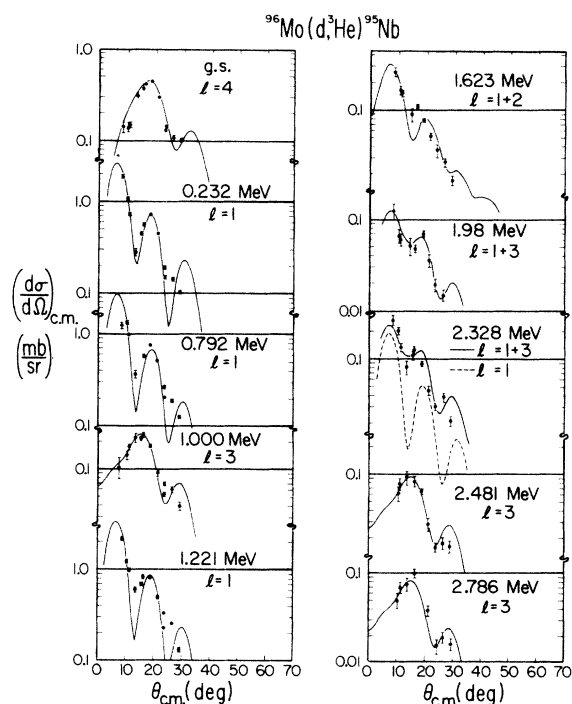


FIG. 2. Angular distributions for the  $^{96}\text{Mo}(d,^3\text{He})^{95}\text{Nb}$  reaction. The errors shown are statistical only. The curves are DWBA calculations for the  $l$  transfers indicated.

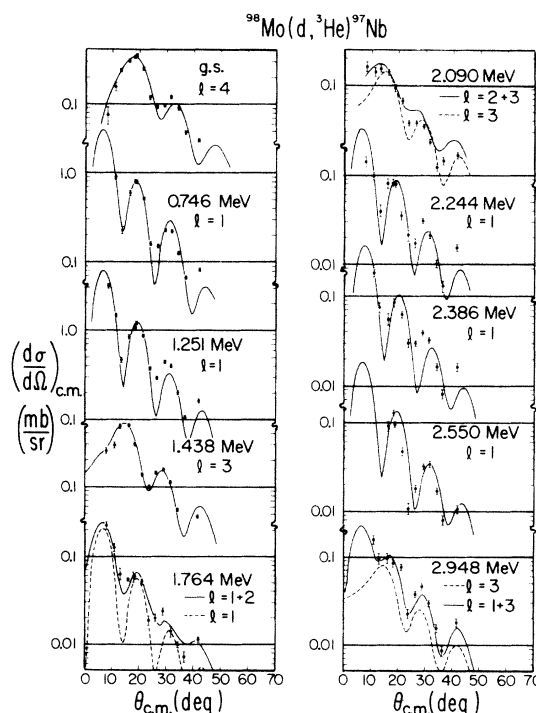


FIG. 3. Angular distributions for the  $^{98}\text{Mo}(d,^3\text{He})^{97}\text{Nb}$  reaction. See Fig. 2 caption.

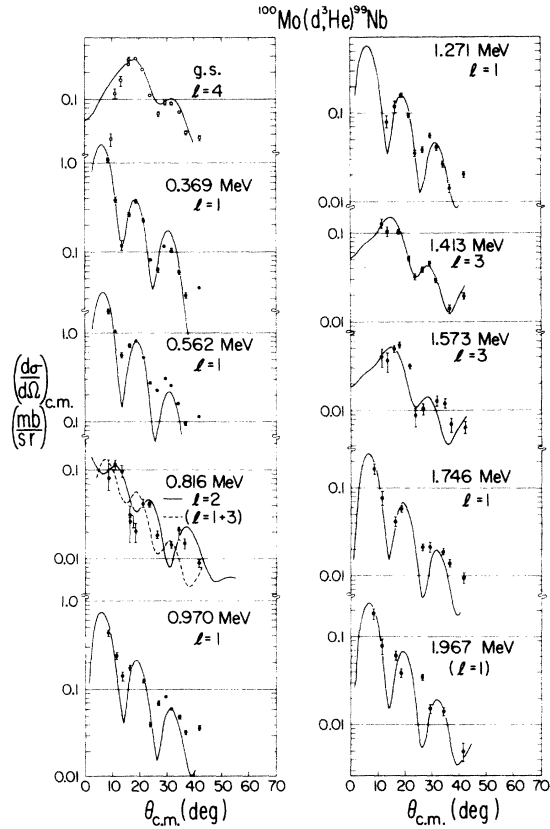


FIG. 4. Angular distributions for the  $^{100}\text{Mo}(d, {}^3\text{He})^{99}\text{Nb}$  reaction. See Fig. 2 caption.

in other communications on the neutron hole states in the Mo isotopes.

All of the data were accumulated in one experimental period. The  $^{100}\text{Mo}$  data were taken between the  $^{98}\text{Mo}$  and  $^{96}\text{Mo}$  runs, and absolute energy calibrations were established for both detector stacks from the  $(d, {}^3\text{He})$  reaction on  $^{98}\text{Mo}$  and  $^{96}\text{Mo}$  as well as on  $^{16}\text{O}$  and  $^{12}\text{C}$  contaminants present in all three Mo targets. The  $Q$  value thus measured for the  $^{100}\text{Mo}(d, {}^3\text{He})^{99}\text{Nb}$  reaction was  $-5.639 \pm 0.015$  MeV, with less than 2 keV spread between results for 10 different angles at which the measurement was made. This results in a mass excess for

$^{99}\text{Nb}$  of  $-82342 \pm 15$  keV which may be compared with the estimated value<sup>13</sup> of  $-82860$  keV. The bulk of the uncertainty is due to inability to reproduce  $Q$  values of known peaks from run to run ( $\pm 10$  keV, primarily in the  $^{15}\text{N}$  and  $^{11}\text{B}$  states) and accumulated uncertainties in the energies of the calibration peaks ( $\pm 5$  keV). Ten groups were identified with each reaction and angular distributions were obtained for laboratory angles from  $8.3$  to  $40.8^\circ$  (Figs. 2–4) with an absolute normalization uncertainty of about 10%.

### III. DISTORTED-WAVE BORN-APPROXIMATION CALCULATIONS

Distorted-wave Born-approximation (DWBA) calculations including finite-range and nonlocal (FRNL) corrections were performed using the computer code DWUCK<sup>14</sup> and optical-model parameters from the literature.<sup>2, 15</sup> These parameters as well as the form factor and FRNL parameters are listed in Table I. The calculated and experimental cross sections are related by

$$\left(\frac{d\sigma}{d\Omega}\right)_{\text{exp}} = \frac{NC^2S}{2J+1} \frac{d\sigma}{d\Omega}_{\text{DWUCK}}, \quad (1)$$

where  $J$  is the transferred angular momentum,  $N$  is the normalization constant determined from the internal structure of the projectiles, and  $C^2S$  is the spectroscopic factor. We have adopted a value of 2.30 for  $N$ .

### IV. EXPERIMENTAL RESULTS

#### A. $^{95}\text{Nb}$

A summary of the experimental results for  $^{95}\text{Nb}$  is given in Table II. Angular distributions and DWBA predictions are shown in Fig. 2. The data are fitted reasonably well for most of the states, but the 1.623, 1.98, and 2.328 MeV states could not be fitted assuming a unique  $l$  value. The angular distribution for the 1.623 MeV state was best fitted with a mixture of  $l=1$  and  $l=2$  transfers. States with these  $l$  assignments were observed at about this energy in the  $({}^3\text{He}, d)$  reaction.<sup>4</sup> The

TABLE I. Optical-model and FRNL parameters used in DWBA calculations (MeV fm units).

Particle	$V$	$r_0$	$a$	$W$	$4W_D$	$r_I$	$a_I$	$r_c$	$V_{so}$	$r_{so}$	$a_{so}$	$\beta^2$ <sup>a</sup>	FNRNG <sup>b</sup>
$d$ <sup>c</sup>	100.8	1.099	0.835		53.64	1.344	0.747	1.3	6.53	1.099	0.835	0.54	0.77
${}^3\text{He}$ <sup>d</sup>	157.8	1.174	0.706	11.71		1.596	1.032	1.4				0.20	
$p$		1.15	0.65				$\lambda_{so}=25$	1.25				0.85	

<sup>a</sup> Nonlocal parameter used in DWUCK.

<sup>b</sup> Finite range parameter for  $(d, {}^3\text{He})$  reactions used in DWUCK.

<sup>c</sup> Reference 15.

<sup>d</sup> Reference 2.

TABLE II. Summary of the experimental results for  $^{95}\text{Nb}$ .

$^{95}\text{Nb}^*$ (MeV $\pm$ keV)	$l_P$	$J^\pi{}^b$	Present work	$C^2S_P$		$^{94}\text{Zr}(^3\text{He}, d)^{95}\text{Nb}^a$	
				Ohnuma and Yntema <sup>c</sup>	$^{95}\text{Nb}^*$ (MeV)	$l_P$	$G_{ij}{}^d$
0.0	4	$\frac{3}{2}^+$	2.54	2.9	0.0	4	7.8
0.232 $\pm$ 5	1	$\frac{1}{2}^-$	1.50	1.6	0.236	1	0.60
					0.728	2	0.84
0.792 $\pm$ 7	1	$\frac{3}{2}^-$	1.74	1.8	0.799	1	0.40
1.000 $\pm$ 8	3	$\frac{5}{2}^-$	1.98	2.1			
1.221 $\pm$ 12	1	$\frac{3}{2}^-$	1.72	2.4	1.223	1	0.12
					1.274	1	0.10
					1.590	2	0.18
					1.645	(1)	(0.14)
1.623 $\pm$ 12	1 + 2	$\frac{3}{2}^-$	0.14		1.810	2	0.18
		$\frac{5}{2}^+$	0.06		1.913	2	0.24
1.98 $\pm$ 25	1 + 3	$\frac{3}{2}^-$	0.07		2.070	2	0.36
		$\frac{5}{2}^-$	0.59		2.121	2	0.42
					2.165	2	0.72
2.328 $\pm$ 12	1 + 3	$\frac{3}{2}^-$	0.14		2.373	(0)	
		$\frac{5}{2}^-$	1.12		2.406	(0 + 2)	
					2.431	(2)	
2.481 $\pm$ 12	3	$\frac{5}{2}^-$	1.17				
2.786 $\pm$ 15	3	$\frac{5}{2}^-$	1.12		2.967	2	0.30

<sup>a</sup>Reference 4.<sup>b</sup> $J^\pi$  values are those which seem most plausible on a shell model basis; no assignments have been made.<sup>c</sup>Reference 1.<sup>d</sup> $G_{ij} = C^2S_{ij}(2J_f + 1)/2J_i + 1$ .

data for the 1.98 and 2.328 MeV states could be fitted by assuming that they were doublets populated by  $l=1$  and  $l=3$  transfers. The results for low-lying states are in good agreement with those of Ohnuma and Yntema<sup>1</sup> obtained at 23 MeV bombarding energy. Most of the expected  $1g_{9/2}$ ,  $2p_{1/2}$ ,  $2p_{3/2}$ , and  $1f_{5/2}$  strength is observed. For the purpose of comparison, we have included results of the  $^{94}\text{Zr}(^3\text{He}, d)^{95}\text{Nb}$  reaction<sup>4</sup> in Table II. None of the states observed in the present experiment above 1.623 MeV in excitation were observed in the ( $^3\text{He}, d$ ) reaction.

B.  $^{97}\text{Nb}$ 

The experimental results for  $^{97}\text{Nb}$  are compared with other studies in Table III. Satisfactory DWBA fits to the angular distributions (Fig. 3) were obtained for most of the levels. The present results differ from those of Ohnuma and Yntema<sup>1</sup> primarily for the 0.746 MeV  $l=1$  and 1.438 MeV  $l=3$  states where the spectroscopic factors we obtain are about a factor of 2 larger. The angular distribution obtained for the  $l=3$  state by Ohnuma and Yntema was rather nondescript and poorly fitted

by the calculation, which could be the source of this discrepancy, but the fits from both experiments to the  $l=1$  first excited state are good.

The states at 1.764 and 2.090 MeV could not be fitted assuming a unique  $l$  value. States assigned  $l=2$  were observed at these energies in the  $^{96}\text{Zr}(^3\text{He}, d)^{97}\text{Nb}$  reaction.<sup>5</sup> The angular distributions for these states could be fitted assuming they were doublets populated by  $l=1$  and  $l=2$  transfers for the 1.764 MeV state and  $l=2$  and  $l=3$  transfers for the 2.090 MeV state. In the studies<sup>16, 17</sup> of  $\beta$  decay of  $^{97}\text{Zr}$  to states in  $^{97}\text{Nb}$ , states

at 1.751 MeV, assigned  $(\frac{5}{2}^+, \frac{7}{2}^+)$ , and at 1.765 MeV, assigned  $(\frac{1}{2}^-, \frac{3}{2}^+)$ , were observed. An assignment of  $l=1+2$  was also made in a study of the  $^{96}\text{Zr}(d, n)^{97}\text{Nb}$  reaction<sup>18</sup> for a state at 1.74 MeV.  $\beta$ -decay work<sup>17</sup> indicates positive parity and a  $J=\frac{1}{2}$  or  $\frac{3}{2}$  assignment for a state at 2.107 MeV while the  $(^3\text{He}, d)$  results<sup>5</sup> indicate  $l=2$  assignments for states at 2.092 and 2.114 MeV.

The  $(\frac{1}{2}^-, \frac{3}{2}^-)$  assignment of Megli *et al.*<sup>16</sup> for the 2.247 MeV state is in agreement with ours. The angular distribution for the group at 2.948 MeV could be best fitted by a mixture of  $l=1$  and  $l=3$

TABLE III. Summary of experimental results for  $^{97}\text{Nb}$ .

$^{97}\text{Nb}^*$ (MeV $\pm$ keV)	$l_P$	$J^\pi$ <sup>b</sup>	$C^2S_p$		$^{96}\text{Zr}(^3\text{He}, d)^{97}\text{Nb}^a$		
			Present work	Ohnuma and Yntema <sup>c</sup>	$^{97}\text{Nb}^*$ (MeV)	$l_P$	$G_{ij}$ <sup>d</sup>
0.0	4	$\frac{9}{2}^+$	2.27	2.2	0.0	4	8.8
0.746 $\pm$ 5	1	$\frac{1}{2}^-$	2.06	1.1	0.746	1	0.27
1.251 $\pm$ 8	1	$\frac{3}{2}^-$	2.43	2.5	1.253	1	0.26
1.438 $\pm$ 9	3	$\frac{5}{2}^-$	5.8	2.5	1.434	(1, 3)	(0.074, 0.031)
					1.554	1	0.024
1.764 $\pm$ 10	1 + 2	$\frac{3}{2}^-$	0.12		1.754	2	0.66
		$\frac{5}{2}^+$	0.06		1.776	(1)	(0.17)
					1.856	2	0.32
					1.945	4	0.37
					2.048	(1)	(0.066)
2.090 $\pm$ 10	2 + 3	$\frac{5}{2}^+$	0.08		2.092	2	0.41
		$\frac{5}{2}^-$	1.0		2.114	(2)	(0.19)
2.244 $\pm$ 10	1	$\frac{3}{2}^-$	0.26				
					2.357	(0, 2)	(0.15, 0.24)
2.386 $\pm$ 12	(1)	$(\frac{3}{2}^-)$	(0.29)				
					2.525	2	0.20
2.550 $\pm$ 20	1	$\frac{3}{2}^-$	0.37				
					2.676	2	0.14
					2.702	2	0.17
					2.727	2	0.29
					2.748	(2)	(0.12)
					2.792	(0)	(0.045)
2.948 $\pm$ 15	1 + 3	$\frac{3}{2}^-$	0.15				
		$\frac{5}{2}^-$	0.98				
					2.981	(0)	(0.03)
					3.067	(2)	(0.12)

<sup>a</sup>Reference 5.

<sup>b</sup>Assumed from shell model consideration.

<sup>c</sup>Reference 1.

<sup>d</sup> $G_{ij} = C^2 S_{ij}(2J_f + 1)/(2J_i + 1)$ .

transfers, as shown in Fig. 3. Essentially all of the expected hole strength is observed, although our measured  $1f_{5/2}$  strength exceeds the sum rule limit but remains within the approximately 20% uncertainties associated with DWBA analyses.

### C. $^{99}\text{Nb}$

Table IV summarizes the experimental results obtained for  $^{99}\text{Nb}$ , while angular distributions obtained are shown in Fig. 4 along with DWBA calculations. The levels of  $^{99}\text{Nb}$  have also been studied by looking at the  $\beta$  decay of  $^{99}\text{Nb}$  itself and of  $^{99}\text{Zr}$  into  $^{99}\text{Nb}$  with subsequent  $\gamma$  emission.<sup>7</sup> The  $\beta$ -decay  $Q$  value obtained for  $^{99}\text{Nb}$  ( $3.7 \pm 0.2$  MeV) leads to a mass excess of  $-82\,260 \pm 200$  keV, in agreement with our value of  $-82\,342 \pm 15$  keV. The energy levels deduced in the two experiments are shown in Fig. 5. The ( $\frac{1}{2}^-$ ) isomeric level referred to by Eidens, Roeckl, and Armbruster<sup>7</sup> would very likely be the 0.369 MeV  $l=1$  level observed in the present experiment. Otherwise there is little apparent overlap between the two experiments. One might postulate that the  $\gamma$  lines involved actually represent transitions between some of the levels observed in the present experiment, if at least one additional level is postulated. However, such schemes would have the decay terminating in the ( $\frac{1}{2}^-$ ) level at 0.369 MeV which has a 2.4 min half-life, whereas data from the fission decay chain<sup>7</sup> indicates that these decays proceed instead to the ground state. The  $\log ft$  values of approximately 4 obtained in the  $\beta$ -decay experiment<sup>7</sup> imply

TABLE IV. Summary of the experimental results for  $^{99}\text{Nb}$ .  $^{100}\text{Mo}(d, ^3\text{He})^{99}\text{Nb}$   $Q = -5.639 \pm 0.015$  MeV; Mass excess  $^{99}\text{Nb} = -82\,342 \pm 15$  keV.

$^{99}\text{Nb}^*$ (MeV $\pm$ keV)	$l_p$	$J^\pi$ <sup>a</sup>	$C^2S_p$
0.0	4	$\frac{3}{2}^+$	2.65
$0.369 \pm 5$	1	$\frac{1}{2}^-$	1.55
$0.562 \pm 5$	1	$\frac{3}{2}^-$	2.52
$0.816 \pm 7$	(1+3)	$\frac{5}{2}^+$	0.16
		$(\frac{3}{2}^-)$	(0.11)
		$(\frac{5}{2}^-)$	(0.72)
$0.970 \pm 10$	1	$\frac{3}{2}^-$	1.0
$1.271 \pm 10$	1	$\frac{3}{2}^-$	0.56
$1.413 \pm 15$	3	$\frac{5}{2}^-$	2.30
$1.573 \pm 12$	3	$\frac{5}{2}^-$	1.00
$1.746 \pm 15$	1	$\frac{3}{2}^-$	0.27
$1.967 \pm 12$	(1)	$(\frac{3}{2}^-)$	(0.27)

<sup>a</sup> Assumed from shell model considerations.

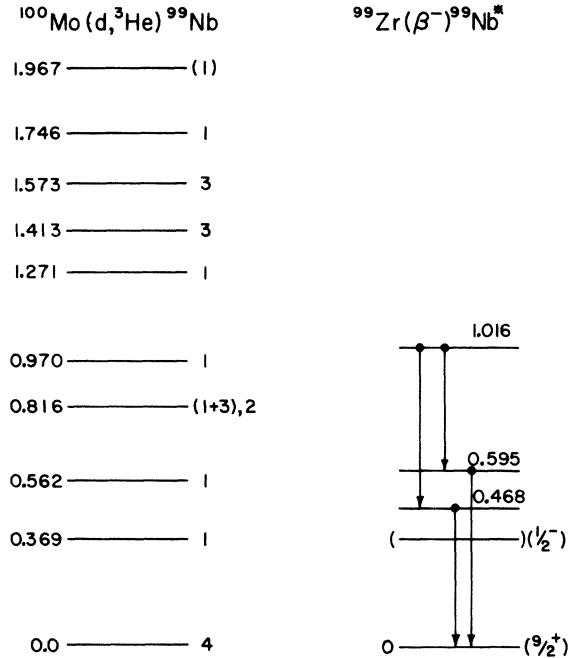


FIG. 5. The  $^{99}\text{Nb}$  levels observed in this reaction are compared with those reported in Ref. 7. The excitation energies are in MeV with  $l$  values obtained in the present study indicated.

an allowed transition which, since the  $^{99}\text{Zr}$  ground state almost certainly has positive parity (no negative parity shell model levels are available for the odd neutron) indicates positive parity for these levels. So it is not surprising that none of these levels were excited with the  $(d, ^3\text{He})$  reaction.

The ground state is fitted well by  $l=4$  transfer while the first two excited states are fitted well by  $l=1$  transfer. The state at 0.816 MeV is best fitted by  $l=2$  transfer. The shape of the theoretical curve obtained by a mixture of  $l=1$  and  $l=3$  transfers would fit the data if the curve is shifted by about  $3^\circ$  (Fig. 4). The levels at 0.970 and 1.271 MeV are fitted well by  $l=1$ , while the states at 1.413 and 1.573 MeV are fitted well by  $l=3$  and represent the major components of the  $\frac{5}{2}^-$  hole strength. The distribution for the 1.573 MeV level appears similar to the ground state but due to  $Q$  dependence is fitted much better by  $l=3$  than  $l=4$ . The states at 1.746 and 1.967 MeV are best

TABLE V. Quasiparticle energies (in MeV) used for calculations.

	$2p_{1/2}$	$2p_{3/2}$	$1f_{5/2}$
$^{95}\text{Nb}$	0.33	1.01	1.90
$^{97}\text{Nb}$	0.85	1.50	1.90
$^{99}\text{Nb}$	0.47	0.70	1.46

fitted by an  $l=1$  transfer, but the quality of the fit for the 1.967 MeV state prevents a definitive assignment. As was the case for  $^{95, 97}\text{Nb}$ , most of the expected hole strength was observed in  $^{99}\text{Nb}$ , although only about half of the available  $1f_{5/2}$  strength was observed.

### V. PARTICLE-CORE-COUPLING MODEL

In a simple minded shell model prescription, one would expect that for the Mo isotopes ( $Z=42$ ), the proton  $2p_{1/2}$ ,  $2p_{3/2}$ , and  $1f_{5/2}$  subshells are completely filled and there would be two protons in the  $1g_{9/2}$  shell. The splitting of the negative parity  $2p_{1/2}$ ,  $2p_{3/2}$ , and  $1f_{5/2}$  states into just a few levels suggests a description where the single-hole states are coupled with the ground and low-lying excited states of the even-even Mo isotopes. The total Hamiltonian  $H$  for the odd-mass nucleus is written as

$$H = H_0 + H_{\text{sp}} + H_{\text{int}}, \quad (2)$$

where  $H_0$  is the core Hamiltonian,  $H_{\text{sp}}$  the single-particle Hamiltonian for the extra nucleon, and  $H_{\text{int}}$  describes the interaction between the extra nucleon and the core.

In the present calculations, we have taken the interaction between the core and the particle given by<sup>19</sup>

$$H_{\text{int}} = \sum_k T_c^k T_p^k, \quad (3)$$

where  $T_c^k$  and  $T_p^k$  are arbitrary spherical tensors of rank  $k$  acting in the spaces of the core and the particle, respectively. Only two terms in this interaction<sup>20</sup> are kept, yielding

$$H_{\text{int}} = -\xi(J_c^{(1)} J_p^{(1)}) - \eta(Q_c^{(2)} Q_p^{(2)}), \quad (4)$$

where  $J$  and  $Q$  are the angular momentum and the mass quadrupole moment operators, respectively. There are three parameters of the model, viz.  $\xi$ , the strength of the dipole-dipole interaction;  $\chi_1$ , defined as  $\eta(0 \| Q_c^{(2)} \| 2)$  and  $\chi_2$ , defined as  $\eta(2 \| Q_c^{(2)} \| 2)$ . In the philosophy of the present model, it is assumed that the detailed structure of the core states is unknown. The reduced matrix elements of  $Q_p^{(2)}$  are evaluated by using harmonic oscillator wave functions with an oscillator parameter given by

$$\nu = 41M/\hbar^2 A^{1/3}. \quad (5)$$

The excitation energies and the wave functions of the odd- $A$  Nb isotopes were obtained by diagonalizing the total Hamiltonian between the basis states  $|\alpha_p J_p, \alpha_c J_c |IM\rangle$ , in which the quasiparticle state  $|\alpha_p J_p\rangle$  is coupled with a core state  $|\alpha_c J_c\rangle$  to a state with total angular momentum  $I$  and  $Z$ -

component  $M$ .

The negative parity levels  $\frac{1}{2}^-$ ,  $\frac{3}{2}^-$ ,  $\frac{5}{2}^-$ ,  $\frac{7}{2}^-$ , and  $\frac{9}{2}^-$  of Nb isotopes were assumed to be given by the coupling of proton holes in the  $2p_{1/2}$ ,  $2p_{3/2}$ , and  $1f_{5/2}$  subshells with the  $0^+$  ground state and the  $2^+$  first excited state of the Mo isotopes. The single-particle energies for the  $2p_{1/2}$ ,  $2p_{3/2}$ , and  $1f_{5/2}$  orbitals used in the calculation are shown in Table V. Since the spectroscopic information obtained here indicates that  $2p$  and  $1f$  orbits are not completely filled, a quasiparticle formalism was used in the present calculations where  $1g_{9/2}$ ,  $2p_{1/2}$ ,  $2p_{3/2}$ , and  $1f_{5/2}$  orbits were assumed to be 30, 70, 80, and 90% full, respectively, for each nucleus. The Hamiltonian matrices for these states were diagonalized to obtain the energy eigenvalues and eigenfunctions by varying the values of  $\xi$ ,  $\chi_1$ , and  $\chi_2$  from 0.0 to 0.5. It was found that the best agreement with the experimental data was obtained with the parameters listed in Table VI. Some of our calculations are with  $\xi=0.0$  implying the dipole-dipole interaction has been turned off. The actual presence of this  $jj$  term in the Hamiltonian is rather questionable. In our calculations, we have found that this term is in general weak and in some cases can be completely neglected leaving only the quadrupole-quadrupole term.

### VI. RESULTS AND DISCUSSION

#### A. $^{95}\text{Nb}$

In Fig. 6, the energy levels obtained in the present experiment are shown in column b with the theoretical predictions in columns a ( $\xi=0.0$ ) and c ( $\xi=0.05$ ). The spin and parity predictions for the first four excited states are in agreement with the experimental data. The spectroscopic factor for the first excited state agrees very well with the predicted value. The spectroscopic factor for the  $l=1$  second excited state at 0.792 MeV is somewhat smaller than that predicted (assuming  $\frac{3}{2}^-$ ), whereas the  $l=1$  fourth excited state (also assumed  $\frac{3}{2}^-$ ) at 1.221 MeV has a larger spectro-

TABLE VI. Parameters for the hole-core coupling model.

Nucleus	Set	$\xi$ (MeV)	$\chi_1$ (MeV fm <sup>-2</sup> )	$\chi_2$ (MeV fm <sup>-2</sup> )
$^{95}\text{Nb}$	A	0.0	0.14	0.090
	B	0.05	0.13	0.080
$^{97}\text{Nb}$	A	0.0	0.14	0.100
	B	0.05	0.13	0.090
$^{99}\text{Nb}$	A	0.0	0.15	0.125
	B	0.10	0.14	0.120

scopic factor than predicted.

There is however a large discrepancy between theory and experiment with the spectroscopic factor for the  $l=3$  (assumed  $\frac{5}{2}^-$ ) state at 1.00 MeV. The state at 1.623 MeV (not fitted very well assuming a unique  $l$ -value assignment) could be associated with the  $\frac{1}{2}^-$  state predicted at 1.8–2.0 MeV. The sixth excited state observed at 1.98 MeV is very weak and could be a composite of the

$^{95}\text{Nb}$

			3.054 $\frac{0.32}{0.016}$ $5/2^-$
			3.002 $\frac{0.016}{0.018}$ $3/2^-$
			2.994 $\frac{0.018}{0.018}$ $1/2^-$
2.933 $\frac{0.45}{0.0}$ $5/2^-$		2.844 $\frac{0.0}{0.0}$ $7/2^-$	
2.882 $\frac{0.0}{0.0}$ $7/2^-$			
	2.786 $\frac{1.12}{0.0}$ 3		
2.726 $\frac{0.26}{0.0}$ $3/2^-$			
2.705 $\frac{0.0}{0.0}$ $9/2^-$			
2.636 $\frac{0.028}{0.028}$ $1/2^-$			
		2.462 $\frac{0.0}{0.0}$ $9/2^-$	
	2.481 $\frac{1.17}{0.0}$ 3		
		2.328 $\frac{0.14}{1.12}$ $1+3$	
		2.068 $\frac{0.092}{1.26}$ $3/2^-$	
		2.041 $\frac{1.26}{0.028}$ $5/2^-$	
		2.034 $\frac{0.028}{3.48}$ $1/2^-$	
2.031 $\frac{1.30}{0.13}$ $5/2^-$	1.980 $\frac{0.07}{0.59}$ $1+3$	1.824 $\frac{3.48}{0.0}$ $5/2^-$	
1.927 $\frac{0.13}{0.0}$ $3/2^-$			
1.844 $\frac{0.0}{3.19}$ $7/2^-$			
1.814 $\frac{3.19}{0.041}$ $5/2^-$			
1.807 $\frac{0.041}{0.041}$ $1/2^-$			
	1.623 $\frac{0.14}{0.06}$ $1+2$	1.698 $\frac{0.0}{0.0}$ $7/2^-$	
		1.360 $\frac{0.61}{0.0}$ $3/2^-$	
1.313 $\frac{0.80}{0.0}$ $3/2^-$			
	1.221 $\frac{1.72}{0.0}$ 1		
		1.090 $\frac{0.35}{0.0}$ $5/2^-$	
1.121 $\frac{0.47}{0.0}$ $5/2^-$			
	1.000 $\frac{1.98}{0.0}$ 3		
		0.873 $\frac{2.49}{0.0}$ $3/2^-$	
0.830 $\frac{2.25}{0.0}$ $3/2^-$	0.792 $\frac{1.74}{0.0}$ 1		
		0.260 $\frac{1.35}{0.0}$ $1/2^-$	
0.236 $\frac{1.33}{0.0}$ $1/2^-$	0.232 $\frac{1.50}{0.0}$ 1		
0.0 $\frac{2.8}{a}$ $9/2^+$	0.0 $\frac{2.54}{b}$ 4	0.0 $\frac{2.8}{c}$ $9/2^+$	
Theo	Expt	Theo	

FIG. 6. Comparison of the experimental energy levels (column b) with the theoretical predictions, column a with parameter set A and column c with set B of Table VI, for  $^{95}\text{Nb}$ . The excitation energies (in MeV) are shown to the left of the lines while the spectroscopic factors are indicated on the line, and  $l_p$  experimental assignments or  $J^\pi$  theoretical predictions are indicated to the right of the line.

$\frac{3}{2}^-$  and  $\frac{7}{2}^-$  states predicted in this energy range.

Next there are three excited  $l=3$  (assumed  $\frac{5}{2}^-$ ) levels, the 2.328 MeV state being a possible doublet with  $l=1$  and  $l=3$ . The predicted  $\frac{5}{2}^-$  levels at about 1.8 and 2.0 MeV have an energy difference approximately the same as the 2.33 and 2.48 MeV  $l=3$  levels, but are predicted much too low in excitation by this model. The third member of this group at 2.786 MeV may correspond to the state predicted at 2.93 MeV for  $\xi=0$  and at a slightly higher energy for  $\xi=0.05$ . There are a few more weak states predicted which would be hard to observe. In general, the model is fairly successful in predicting  $l=1$  states, but fails to predict the energies and spectroscopic factors for some of the  $l=3$  levels.

$^{97}\text{Nb}$

			2.948 $\frac{0.15}{0.98}$ $1+3$	2.970 $\frac{0.37}{0.04}$ $5/2^-$
				2.908 $\frac{0.04}{0.03}$ $3/2^-$
				2.884 $\frac{0.03}{0.0}$ $1/2^-$
				2.759 $\frac{0.0}{0.0}$ $7/2^-$
			2.852 $\frac{0.52}{0.0}$ $5/2^-$	
			2.796 $\frac{0.0}{0.0}$ $7/2^-$	
			2.645 $\frac{0.82}{0.0}$ $3/2^-$	
			2.597 $\frac{0.0}{0.054}$ $9/2^-$	
			2.533 $\frac{0.054}{0.0}$ $1/2^-$	
				2.550 $\frac{0.37}{0.0}$ 1
				2.453 $\frac{0.09}{0.03}$ $3/2^-$
				2.419 $\frac{0.03}{0.16}$ $1/2^-$
				2.402 $\frac{0.16}{0.0}$ $5/2^-$
				2.355 $\frac{0.0}{0.0}$ $9/2^-$
			2.389 $\frac{0.16}{0.12}$ $5/2^-$	
			2.386 (0.29) (1)	
			2.304 $\frac{0.12}{0.0}$ $3/2^-$	
			2.228 $\frac{0.0}{0.046}$ $7/2^-$	
			2.188 $\frac{0.046}{0.0}$ $1/2^-$	
				2.244 $\frac{0.26}{0.0}$ 1
				2.090 $\frac{0.08}{1.0}$ $2+3$
				2.083 $\frac{0.0}{0.0}$ $7/2^-$
			1.934 $\frac{3.20}{0.0}$ $5/2^-$	
				1.919 $\frac{3.69}{0.0}$ $5/2^-$
			1.754 $\frac{0.98}{0.06}$ $3/2^-$	1.764 $\frac{0.12}{0.06}$ $1+2$
				1.796 $\frac{0.78}{0.0}$ $3/2^-$
			1.453 $\frac{1.52}{0.0}$ $5/2^-$	1.438 $\frac{5.8}{0.0}$ 3
				1.445 $\frac{1.19}{0.0}$ $5/2^-$
				1.337 $\frac{2.29}{0.0}$ $3/2^-$
			1.285 $\frac{2.02}{0.0}$ $3/2^-$	1.251 $\frac{2.43}{0.0}$ 1
			0.733 $\frac{1.30}{0.0}$ $1/2^-$	0.746 $\frac{2.06}{0.0}$ 1
				0.765 $\frac{1.34}{0.0}$ $1/2^-$
0.0 $\frac{2.8}{a}$ $9/2^+$	0.0 $\frac{2.27}{b}$ 4	0.0 $\frac{2.8}{c}$ $9/2^+$		
Theo	Expt	Theo		

FIG. 7. Comparison of the experimental data with the theoretical predictions for  $^{97}\text{Nb}$ . See Fig. 6 caption.

B.  $^{97}\text{Nb}$ 

Theoretical and experimental results for  $^{97}\text{Nb}$  are shown in Fig. 7. Both calculations are in remarkable agreement with the experimental data for the first five excited energy levels except for the spectroscopic factors for some of the states. As indicated earlier, the sum of the spectroscopic factors for the  $l=3$  states is higher than what one expects from the sum rule. The predicted spectroscopic factors for the first two  $l=1$  states are in reasonable agreement with the experimental numbers. The spectroscopic factors for the  $l=3$  states at 1.44 and 2.09 MeV are interchanged in the theory relative to the data. The  $l=1$  state at 1.76 MeV is much weaker than predicted. The next three  $l=1$  states are observed with small spectroscopic factors. For  $\xi=0.0$  three  $l=1$  states are predicted at almost the energies corresponding to the experimental energies with small spectroscopic factors. With  $\xi=0.05$  this feature is not reproduced. The highest experimental level observed (2.948 MeV) is a possible doublet with a mixture of  $l=1$  and  $l=3$ . Calculations with  $\xi=0.0$  predict an  $l=3$ ,  $J^\pi = \frac{5}{2}^-$  level at 2.85 MeV with a spectroscopic factor in reasonable agreement with the  $l=3$  component for this state. On the other hand, the calculations with  $\xi=0.05$  predict two  $l=1$  states and one  $l=3$  state in the 2.90–2.96 MeV region with spectroscopic factors in fair agreement with the experimental data.

C.  $^{99}\text{Nb}$ 

The results for  $^{99}\text{Nb}$  are presented in Fig. 8. This nucleus has been the subject of an earlier communication,<sup>11</sup> so we shall discuss it only briefly. The calculations in column c ( $\xi=0.1$ ) are taken from Ref. 11. Calculations with  $\xi=0.0$  and  $\xi=0.1$  predict a  $\frac{5}{2}^-$  level at about 0.8 MeV. A level at 0.816 MeV is best fitted by  $l=2$  transfer, but as pointed out in Sec. IV C an  $l=3$  component cannot be completely ruled out. The calculation with  $\xi=0.0$  predicts the presence of a  $\frac{3}{2}^-$  level at 1.12 MeV with  $C^2S=0.79$  which agrees with the  $l=1$  state observed at 0.970 MeV with  $C^2S=1.0$ . The  $\xi=0.1$  calculation predicts in this region only a  $\frac{7}{2}^-$  state (at 0.95 MeV) which should not be excited strongly. Otherwise, on the whole, the calculations with  $\xi=0.1$  seem to be superior to those with  $\xi=0.0$ .

## D. Predictions for the quadrupole moments

The parameters listed in Table VI show a very consistent trend for the three nuclei. The value of  $\chi_2$  decreases from  $^{99}\text{Nb}$  to  $^{95}\text{Nb}$  showing a smaller quadrupole moment for  $^{96}\text{Mo}$  compared to  $^{100}\text{Mo}$ . Using the values of the transitional probabilities

$B(E2, 0^+ \rightarrow 2^+)$  for Mo isotopes<sup>21</sup> and the corresponding values of  $\chi_1$  and  $\chi_2$  from Table VI, the absolute value of the spectroscopic quadrupole moments of the first  $2^+$  level in  $^{96}\text{Mo}$ ,  $^{98}\text{Mo}$ , and  $^{100}\text{Mo}$  are 0.26, 0.29, and 0.47 b, respectively. These values lie between the predictions using the collective vibrational model and the rotational model. The former model predicts 0.0 b for all the three Mo isotopes whereas the latter model gives  $|Q_{2^+}| = 0.483, 0.484, \text{ and } 0.657 \text{ b}$  for  $^{96}\text{Mo}$ ,  $^{98}\text{Mo}$ , and  $^{100}\text{Mo}$ , respectively.

## VII. CONCLUSIONS

The energy level scheme for the proton hole states for  $^{95}\text{Nb}$ ,  $^{97}\text{Nb}$ , and  $^{99}\text{Nb}$  are obtained by the ( $d, ^3\text{He}$ ) reaction. The results for low-lying levels in  $^{95}\text{Nb}$  and  $^{97}\text{Nb}$  agree with those obtained by Ohnuma and Yntema<sup>1</sup>; however, the spectroscopic factors for  $^{97}\text{Nb}$  are larger and several new levels are observed at higher excitation. For  $^{99}\text{Nb}$ , we observe nine new levels which appear to be different from the levels obtained in the study of  $\beta$  decay<sup>7</sup> of  $^{99}\text{Zr}$  and  $^{99}\text{Nb}$  which probably popu-

$^{99}\text{Nb}$		
		2.510 $\frac{0.04}{\sqrt{0.03}} \frac{1}{2}^-$ 2.490 $\frac{0.44}{0.44} \frac{3}{2}^-, \frac{5}{2}^-$
2.245 $\frac{0.83}{0.0} \frac{5}{2}^-$		
2.159 $\frac{0.0}{0.0} \frac{7}{2}^-$		2.102 $\frac{0.0}{0.0} \frac{7}{2}^-$
1.956 $\frac{0.069}{0.0} \frac{3}{2}^-$	1.967 $\frac{0.27}{0.27} (1)$	
1.909 $\frac{0.0}{0.0} \frac{9}{2}^-$		
1.839 $\frac{0.093}{0.093} \frac{1}{2}^-$	1.746 $\frac{0.27}{0.27} 1$	1.655 $\frac{0.11}{0.06} \frac{3}{2}^-$ 1.649 $\frac{0.06}{0.06} \frac{1}{2}^-$ 1.554 $\frac{2.03}{2.03} \frac{5}{2}^-$
1.524 $\frac{2.16}{2.16} \frac{5}{2}^-$	1.573 $\frac{1.0}{1.0} 3$	1.554 $\frac{2.03}{2.03} \frac{5}{2}^-$
1.376 $\frac{1.33}{0.21} \frac{5}{2}^-$	1.413 $\frac{?}{?} 3$	1.413 $\frac{0.0}{2.20} \frac{9}{2}^-$ 1.384 $\frac{0.0}{2.20} \frac{5}{2}^-$
1.248 $\frac{0.0}{0.13} \frac{7}{2}^-$	1.271 $\frac{0.56}{0.56} 1$	1.231 $\frac{0.53}{0.53} \frac{3}{2}^-$
1.231 $\frac{0.13}{0.79} \frac{1}{2}^-$		
1.122 $\frac{0.79}{0.79} \frac{3}{2}^-$	0.970 $\frac{1.0}{1.0} 1$	0.951 $\frac{0.0}{0.0} \frac{7}{2}^-$
0.837 $\frac{1.09}{1.09} \frac{5}{2}^-$	0.816 $\frac{(0.11, 0.72)}{0.16} (1+3)$	0.792 $\frac{0.72}{0.72} \frac{5}{2}^-$
0.530 $\frac{2.14}{2.14} \frac{3}{2}^-$	0.562 $\frac{2.52}{2.52} 1$	0.606 $\frac{2.54}{2.54} \frac{3}{2}^-$
0.277 $\frac{1.18}{1.18} \frac{1}{2}^-$	0.369 $\frac{1.55}{1.55} 1$	0.356 $\frac{1.30}{1.30} \frac{1}{2}^-$
0.0 $\frac{2.8}{2.8} \frac{9}{2}^+$	0.0 $\frac{2.65}{2.65} 4$	0.0 $\frac{2.8}{2.8} \frac{9}{2}^+$
a Theo	b Expt	c Theo

FIG. 8. Comparison of the experimental data with the theoretical predictions for  $^{99}\text{Nb}$ . See Fig. 6 caption.

lated only positive parity levels. Most of the expected  $1g_{9/2}$ ,  $2p_{1/2}$ ,  $2p_{3/2}$ , and  $1f_{5/2}$  strengths have been observed in each of three Nb nuclei except for  $^{99}\text{Nb}$  where only about half of the expected  $1f_{5/2}$  strength was observed. A small  $l_p = 2$  strength is observed in each of the Nb isotopes indicating that the proton configurations in the Mo ground states have a small  $2d_{5/2}$  admixture.

The energies and the  $J^\pi$  values for the low-lying states in these nuclei are predicted rather well by a core-coupling model using a quasiparticle formalism. However, the spectroscopic factors for some of the states in  $^{95}\text{Nb}$  and  $^{97}\text{Nb}$  are not predicted well and some of the  $\frac{5}{2}^-$  states in  $^{95}\text{Nb}$  are not well re-

produced. The agreement with  $^{99}\text{Nb}$  is very good. The predicted spectroscopic quadrupole moments for the  $2^+$  state are about 72% of the rotational model limit for  $^{100}\text{Mo}$ , 61% for  $^{98}\text{Mo}$ , and 53% for  $^{96}\text{Mo}$ . This indicates that perhaps  $^{96,98,100}\text{Mo}$  form a series of transitional nuclei leading to a new deformation region around  $A = 104-106$  in agreement with Taketani *et al.*<sup>6</sup>

#### ACKNOWLEDGMENTS

The authors wish to thank Dr. P. H. Hoffmann-Pinther and Dr. T. Kishimoto for several discussions, and R. Weber for his assistance in taking and analyzing the data.

†Work supported in part by the National Science Foundation and the Robert A. Welch Foundation.

\*Present address: Department of Chemistry, Columbia University, New York, N. Y. 10027

<sup>1</sup>H. Ohnuma and J. L. Yntema, *Phys. Rev.* **176**, 1416 (1968).

<sup>2</sup>R. L. Kozub and D. H. Youngblood, *Phys. Rev. C* **4**, 535 (1971) and references therein.

<sup>3</sup>B. M. Preedom, E. Newman, and J. C. Hiebert, *Phys. Rev.* **166**, 1156 (1968).

<sup>4</sup>L. R. Medsker and D. J. Horen, *Nucl. Data* **B8**, 29 (1972).

<sup>5</sup>L. R. Medsker, *Nucl. Data* **B10**, 1 (1973).

<sup>6</sup>H. Taketani, M. Adachi, M. Ogawa, K. Ashibe, and T. Hattori, *Phys. Rev. Lett.* **27**, 520 (1971).

<sup>7</sup>J. Eidens, E. Roeckl, and P. Armbruster, *Nucl. Phys.* **A141**, 289 (1970).

<sup>8</sup>R. L. Kozub and D. H. Youngblood, *Phys. Rev. C* **7**, 410 (1973).

<sup>9</sup>K. H. Bhatt and J. B. Ball, *Nucl. Phys.* **63**, 286 (1965).

<sup>10</sup>J. Vervier, *Nucl. Phys.* **75**, 17 (1966).

<sup>11</sup>P. K. Bindal and D. H. Youngblood, *Phys. Rev. C* **9**,

1618 (1974).

<sup>12</sup>T. Kishimoto, P. K. Bindal, and D. H. Youngblood, to be published.

<sup>13</sup>A. H. Wapstra and N. B. Gove, *Nucl. Data* **A9**, 267 (1971).

<sup>14</sup>Received from P. D. Kunz, University of Colorado.

<sup>15</sup>C. M. Perey and F. G. Perey, *Phys. Rev.* **152**, 923 (1966).

<sup>16</sup>D. G. Megli, G. P. Agin, V. R. Potnis, and C. E. Mandeville, *Z. Phys.* **234**, 95 (1970).

<sup>17</sup>K. J. Hofstetter and T. T. Sugihara, *Nucl. Phys.* **A140**, 658 (1970).

<sup>18</sup>J. L. Horton, C. L. Hollas, P. J. Riley, S. A. S. Zaidi, C. M. Jones, and J. L. C. Ford, Jr., *Nucl. Phys.* **A190**, 362 (1972).

<sup>19</sup>A. deShalit, *Phys. Rev.* **122**, 1530 (1960).

<sup>20</sup>V. K. Thankappan and W. W. True, *Phys. Rev.* **137**, B793 (1965).

<sup>21</sup>J. Barrette, M. Barrette, A. Boutard, R. Haroutunian, G. Lamoureux, and S. Monaro, *Phys. Rev. C* **6**, 1339 (1972).